Colocalization of Heparin and Receptor Binding Sites on Keratinocyte Growth Factor†

Peter J. Kim,‡ Kazuyasu Sakaguchi,§ Hiroshi Sakamoto,§ Carl Saxinger,|| Regina Day,‡ Peter McPhie,⊥ Jeffrey S. Rubin,‡ and Donald P. Bottaro*,‡

Laboratories of Cellular and Molecular Biology, Cell Biology, and Tumor Cell Biology, National Cancer Institute, and Laboratory of Biochemistry and Metabolism, National Institute of Diabetes and Digestive and Kidney Diseases, National Institutes of Health, Bethesda, Maryland 20892

Received January 26, 1998; Revised Manuscript Received March 24, 1998

ABSTRACT: Keratinocyte growth factor (KGF) is a member of the fibroblast growth factor (FGF) family. FGFs are also known as heparin-binding growth factors because they bind to heparin and their physical and biological properties are modulated by heparin. Consistent with a role as a paracrine effector, KGF is produced by cells of mesenchymal origin but is active primarily, if not exclusively, on epithelial cells. KGF is involved in a variety of physiological processes, including proliferation, differentiation, wound healing, and cytoprotection. To identify regions in KGF that contribute to heparin and tyrosine kinase receptor interactions, nine peptides spanning defined motifs in the predicted structure of KGF were synthesized, and their heparin and receptor binding properties were analyzed. Peptides at the amino and carboxyl termini bound heparin, and one peptide showed relative binding comparable to that of KGF. Competitive binding studies showed that this peptide along with two other overlapping peptides specifically displaced KGF bound to the KGF receptor. These three peptides were also selectively recognized by a neutralizing monoclonal antibody against KGF, though only in the presence of heparin. Together, these data suggest that the sites for heparin and receptor binding both reside in the amino and carboxyl termini of KGF, which are spatially juxtaposed in the predicted three-dimensional structure of this molecule.

Keratinocyte growth factor (KGF)[1] is a fibroblast growth factor (FGF) family member that participates in embryonic development and adult homeostasis by stimulating cell proliferation, migration, and differentiation (*1*−*3*). It is produced by cells of mesenchymal origin and exerts its effects primarily on cells of epithelial origin by signaling through a specific receptor tyrosine kinase (*1*, *4*−*6*). This epithelial specificity, determined by tissue-specific splicing of the FGF receptor-2 (FGFR-2) gene to yield a KGF-binding isoform of FGFR2 (KGFR; *7*), is shared also by FGF-10 (*8*, *9*). Although KGF and FGF-10 have overlapping activities in vitro, they appear to have distinct expression patterns during development, as observed in embryonic lung (*6*, *10*−*12*).

In addition to its role as a mediator of normal mesenchymal−epithelial interaction, KGF has been implicated in certain pathological conditions. The increased KGF expression associated with inflammatory bowel disease may be part of a tissue repair response (*13*, *14*), but in other instances KGF may be a primary contributor to disease progression, such as in benign prostatic hypertrophy and prostate cancer (*15*−*17*). The widespread involvement of KGF in normal and disease processes provides a strong impetus to uncover the structural basis of KGF signaling.

All well-characterized FGFs, including KGF, bind heparin, and heparin modulates the ability of the FGFs to signal through their high-affinity tyrosine kinase receptors (*18*−*28*). Several studies have demonstrated the importance of heparin in FGF action, and within the past few years much progress has been made toward identifying the determinants of heparin binding on FGF molecules and understanding the mechanisms by which heparin modulates FGF signaling (*26*−*32*). To identify the receptor and heparin binding sites on KGF, we adopted an approach similar to one used almost a decade ago by Baird and co-workers to identify biologically important regions of basic FGF (bFGF, FGF-2; *33*). In that study, the heparin binding and biological properties of a large number of synthetic bFGF peptides were examined. Two different peptides with mitogenic and heparin binding activities were identified that, in retrospect, corresponded to discrete domains of the bFGF crystallographic structure

† P.J.K. is a National Institutes of Health Research Scholar of the Howard Hughes Medical Institute.

* To whom correspondence should be addressed: Laboratory of Cellular and Molecular Biology, National Cancer Institute, Building 37, Room 1E24, 9000 Rockville Pike, Bethesda, MD 20892. Telephone: (301) 496-4265. Fax: (301) 496-8479. E-mail: dbottaro@helix.nih.gov.

‡ Laboratory of Cellular and Molecular Biology, National Cancer Institute.

§ Laboratory of Cell Biology, National Cancer Institute.

|| Laboratory of Tumor Cell Biology, National Cancer Institute.

⊥ Laboratory of Biochemistry and Metabolism, National Institute of Diabetes and Digestive and Kindey Diseases.

[1] Abbreviations: FGF, fibroblast growth factor; KGF, keratinocyte growth factor; KGFR, KGF receptor; HPLC, high-performance liquid chromatography; PBS, phosphate-buffered saline; SDS, sodium dodecyl sulfate; b-heparin, biotin−heparin conjugate; PNPP, *p*-nitrophenyl phosphate; ELISA, enzyme-linked immunosorbent assay; TAPS, PBS, 0.05% Tween 20, and 0.02% sodium azide; RT, room temperature; PVDF, polyvinylidine difluoride; BSA, bovine serum albumin; DMEM, Dulbecco's Modified Eagle's Medium; HEPES, 4-(2-hydroxyethyl)-1-piperazineethanesulfonic acid.

S0006-2960(98)00191-3
Published on Web 00/00/0000 PAGE EST: 9.8

reported several years later (*34*, *35*); each of these peptides spanned one-third of a protein structure with 3-fold symmetry, known as the β-trefoil fold (*34*−*36*). The β-trefoil fold is shared by bFGF, aFGF, IL-1β, and the Kunitz family of protease inhibitors, proteins with remarkably little overall sequence similarity (*36*). In this structure a six-stranded β-barrel is capped by three pairs of antiparallel β-hairpin loops, and the axis of symmetry is aligned with the long axis of the barrel. The motif BHHB is repeated three times from amino to carboxyl terminus in the amino acid sequence, where B is a single strand of the six-stranded barrel and H is one-half of a hairpin loop (*36*). The only major sequence requirements are three large or medium hydrophobic residues in each of the six barrel strands.

The synthetic peptide strategy used in this study was based on two assumptions: (1) that KGF protein also exhibited the β-trefoil fold, and (2) that peptides corresponding to one-third of the fold may have ordered structure, and thus resemble a portion of the full-length protein surface. We began our study by creating a theoretical three-dimensional (3D) model of the KGF structure based on its sequence identity with bFGF. We then synthesized nine overlapping peptides that each spanned a defined structural motif. The heparin binding properties of the peptides were compared by immobilizing the peptides and measuring their ability to bind biotinylated heparin, and by observing their retention time on a heparin−TSK affinity column. Receptor binding was assayed directly by [^{125}I]KGF competitive binding experiments, and indirectly localized by testing for recognition of the peptides by a KGF-specific neutralizing monoclonal antibody. The structure and conformational changes in the peptides were investigated by circular dichroism (CD) spectroscopy.

EXPERIMENTAL PROCEDURES

Materials. Reagents for peptide synthesis were obtained from Applied Biosystems, Inc., Fluka, and Nova Biochemicals. Heparin purified from porcine intestine was obtained from Fisher. Neutralizing monoclonal anti-KGF antibody 1G4 (*37*) was prepared using conventional methods. Recombinant KGF and bFGF were expressed in bacteria and purified as described previously for KGF (*20*). [^{125}I]KGF was prepared as described previously (*38*). Heparin was biotinylated using photoactivatable biotin from Pierce Chemical Co. as described below.

Peptide Synthesis. Two different methods of peptide synthesis were used in this study. One group of peptides (K1−9, B1, and B2) were prepared with a Perkin-Elmer/Applied Biosystems model 431A peptide synthesizer using small-scale FastMoc chemistry. Cleavage of peptides from the resin and removal of the side-chain protecting groups were carried out using reagent K (*39*). Peptides were purified by reverse phase HPLC on a C-8 column (Vydac) with 0.05% TFA/water/acetonitrile. The mass of peptides was confirmed by electrospray ionization mass spectrometry on a Finnigan MAT SSQ 7000 mass spectrometer. Peptides K1−9, B1, and B2 correspond to amino acid sequences from KGF and bFGF, respectively, as defined in Table 1.

A second group of peptides, each 18 residues long, was synthesized directly in the wells of special 96-well plates as described previously (*40*). These peptides were permanently bound to the plate surface, and the plates were used only for the heparin binding ELISA. Each well contained a different peptide whose starting and ending sites were defined by shifting an 18-residue frame sequentially through the amino acid sequence of KGF (or bFGF) two residues at a time. On the abscissa of Figure 3, position number refers to the peptide sequence starting position within the β-trefoil. The peptide at position 0 starts at Gly62 and ends at Ile79 for KGF, and starts at Ile26 and ends at Ile43 for bFGF. After position 112, the peptide sequences wrapped around to the amino terminus in the same manner as peptides K8 and K9. Another 96-well plate contained peptides from a specific region in the C terminus of KGF or bFGF, and alanine substitutions for selected residues in these regions, as explained in Results.

Table 1

peptide	position[a]	sequence[b]	HTAC retention time (min)
KGF	31−194	ACN...AIT	41
K1	64−103	IRV...RTV	19
K2	70−113	FCR...ESE	ND[c]
K3	95−131	YNI...AKK	5
K4	105−145	GIV...LIL	5
K5	116−155	EFY...SAK	5
K6	137−178	DCN...RGK	5
K7	148−194	YNT...AIT	38
K7a	157−186	THN...QKT	20
K7b	157−194	THN...AIT	26
K7c	148−186	YNT...QKT	32
K8	162−72	EMF...FCR	34
K9	185−89	TAH...GTQ	30
B1	35−79	YCK...KGV	30
B2	114−157	YNT...AKS	26

[a] Position refers to the KGF numbering scheme of Finch et al. (*2*) or the bFGF numbering scheme of Zhu et al. (*35*). [b] Sequence shows the first and last three residues of the amino acid sequence encompassed by the peptide (or protein) from KGF (or bFGF) using standard single-letter code. [c] ND indicates that the heparin−TSK affinity chromatography (HTAC) retention time was not determined.

Heparin−TSK Affinity Chromatography. Retention of KGF and purified peptides by heparin−TSK was measured using a Heparin-5PW column (7.5 mm inside diameter × 7.5 cm, flow rate of 1 mL/min; TosoHaas) on a Waters 600 HPLC. The column was equilibrated in phosphate-buffered saline (pH 7.4) containing 150 mM NaCl, and samples were eluted with a linear gradient of increasing NaCl concentration reaching a maximum of 1.5 M NaCl in 1 h at room temperature. Elution was monitored by UV absorbance at 200−300 nm using a Waters 996 photodiode array detector. Peptide or protein elution was verified by collecting 1 min fractions, aspirating these through PVDF membrane using a dot blot apparatus, and staining the membrane with colloidal Coomassie Blue (Novex). Retention times listed in Table 1 represent the maximum eluted absorbance at 214 or 280 nm (depending on the amino acid composition of the sample) that coincided with positive Coomassie Blue staining.

Heparin Binding ELISA. Photoactivatable biotin (in distilled water) was added to heparin [10 mg/mL in phosphate-buffered saline (PBS); final volume of 3 mL] to a final concentration of 1 mM, and the reaction mixture was placed on a flat polypropylene plate. The plate was UV irradiated in a Stratalinker (Stratagene) at maximum intensity until dry (∼1 h). The dried biotin−heparin (b-heparin)

residue was resuspended in distilled water to a concentration of 2 mg/mL and stored at 4 °C. The elution of KGF from heparin−Sepharose occurred at approximately the same NaCl concentration as elution of KGF from b-heparin immobilized on streptavidin−Sepharose, suggesting that the KGF−heparin interaction was not adversely affected by heparin biotinylation (data not shown).

Peptides K1−9, B1, and B2 (50 μL of a 1.2 μg/mL solution) were adsorbed onto polyvinyl 96-well microtiter plates (Falcon no. 3912) for 1 h at 37 °C in PBS. The wells were washed with PBS, 0.05% Tween 20, and 0.02% sodium azide (TAPS), blocked with TAPS and 0.5% nonfat dry milk for 15 min at 37 °C, and then washed again. Wells were incubated with b-heparin (200 ng/mL) in blocking solution (with or without unlabeled heparin) for 2 h at room temperature (RT). After being washed with TAPS, wells were extracted with various concentrations of NaCl where appropriate, and then incubated with streptavidin−alkaline phosphatase conjugate (500 ng/mL) in blocking solution for 1 h at RT. After the wells were washed with TAPS, bound alkaline phosphatase was detected by incubating each well with 13 mM *p*-nitrophenyl phosphate (PNPP) in 1 mM $MgCl_2$ (pH 9.8) and monitoring the absorbance at 405 nm with an ELISA scanner (BioRad Laboratories) over a 2 h period. Shorter (18mer) peptides synthesized directly in the wells of special 96-well plates were probed with b-heparin similarly, except that the protocol began by blocking with PBS containing 0.5% bovine serum albumin (BSA), 0.1% Tween 20, 0.1% sodium dodecyl sulfate (SDS), and 0.1% Nonidet p-40 for 1 h at RT. Each well was then incubated with b-heparin in this blocking solution for 2 h, and all subsequent steps were as described for peptides K1−9, B1, and B2.

[^{125}I]KGF Binding Assay. Interaction between peptides K1−9, B1, or B2 and the KGFR was evaluated using competitive [^{125}I]KGF binding assays (*38*). NIH3T3 fibroblasts overexpressing the KGFR were subcultured into fibronectin-coated 48-well tissue culture plates and grown to confluence in Dulbecco's Modified Eagle's Medium (DMEM) and 10% calf serum. After being rinsed with DMEM, each well was incubated with 200 μL of DMEM containing 0.5% BSA, 50 mM HEPES (pH 7.4), heparin (1 μg/mL final concentration), and 40 kcpm of [^{125}I]KGF. After peptide or growth factor competitor was added, the plates were incubated for 4 h at 15 °C. The wells were then washed three times with ice-cold PBS, and bound tracer was extracted with 0.5% SDS and detected by γ-counting.

1G4 Binding ELISA and Dot Blot. Recognition of peptides K1−9, B1, or B2 by the KGF-neutralizing monoclonal antibody 1G4 was measured by adsorbing the peptides to polyvinyl 96-well microtiter plates as described above. The neutralizing anti-KGF monoclonal antibody 1G4 (1 μg/mL) was substituted for b-heparin in the same ELISA protocol, followed by three TAPS washes, incubation with 200 ng/mL goat anti-mouse antibody−alkaline phosphatase conjugate (Pierce), three more TAPS washes, and detection of bound secondary antibody after PNPP addition by monitoring absorbance at 405 nm over 2 h. A second system of detecting 1G4−peptide interaction consisted of immobilizing the peptides on polyvinylidine difluoride (PVDF) by aspiration through a dot blot apparatus (Schleicher and Schuell). The PVDF membrane was then removed and processed for 1G4 recognition as follows. The membrane was blocked with PBS, 0.5% Tween 20, and 3% nonfat dry milk for 15 min at RT and washed with PBS. The membrane was then incubated with 1G4 and various concentrations of heparin in PBS and 0.1% BSA for 1 h at RT, washed with PBS, and bound antibody was detected by chemiluminescence (ECL, Amersham).

Structural Analysis of Peptides. Circular dichroism (CD) spectra (190−260 nm) of KGF peptides were measured in a Jasco J500-C spectropolarimeter over a range of heparin concentrations. In control experiments, CD spectra of similar concentrations of heparin alone were measured and the reported spectra for the peptides were corrected for these small contributions. The data are reported as mean residue ellipticity [[(millidegrees) × 10MRW]/[path length (in centimeters) × concentration (in milligrams per milliliter) × 100]]. Typical peptide concentrations were 0.1 mg/mL, in a 0.1 cm path length cell. The mean residue weight (MRW) was assumed to be 110. An increase in measured deflection around 215−220 nm was taken to indicate formation of β-structure in the peptides.

RESULTS

Theoretical 3D Structure of KGF and Synthetic Peptide Design. Both aFGF and bFGF show significant amino acid sequence identity with KGF [37 and 39%, respectively (*2*)]. A region corresponding to the N terminus of KGF (amino acids 1−54), including the signal peptide, is not found in either aFGF or bFGF, so sequence identity between these FGFs is confined to KGF residues 55−194. Sequence alignment of these FGFs indicates that identity is highest in regions that are critical for formation of the β-trefoil fold (*36*). Based on this sequence identity, a theoretical 3D model of KGF was created using the spatial coordinates from the crystal structure of bFGF[2] and the computer program LOOK (Molecular Applications Group, Palo Alto, CA; Figure 1A,B). The first 29 residues of bFGF were not resolved in the crystal structure and the corresponding regions of KGF (residues 1−63) do not align with defined motifs in the β-trefoil fold, so these residues were omitted from the 3D model. It is noteworthy that N-terminally truncated mutants of KGF, extending as far as residue 59, retain potent biological activity and heparin binding, while longer truncations that would disrupt the first barrel strand in the predicted KGF structure obliterate mitogenic activity (*20*). As in bFGF, the structurally resolved portion of the amino terminus and the carboxyl terminus are adjacent in the 3D structure, forming one-third of the six-stranded β-barrel (Figure 1A,B).

Using the KGF−bFGF sequence alignment and the theoretical 3D model of KGF structure, the borders of the B and H strands of the β-trefoil fold were predicted for KGF. Nine peptides corresponding to the human KGF amino acid sequence, designated K1−9, were synthesized, each spanning one-third of KGF and corresponding to one of three structural motifs: BHHB, HHBB, and BBHH (Figure 1C and Table 1). In the predicted structure of KGF two barrel strands and two hairpins of each motif form two separate antiparallel

[2] Protein Data Bank (PDB), Brookhaven National Laboratory, file 1bas.

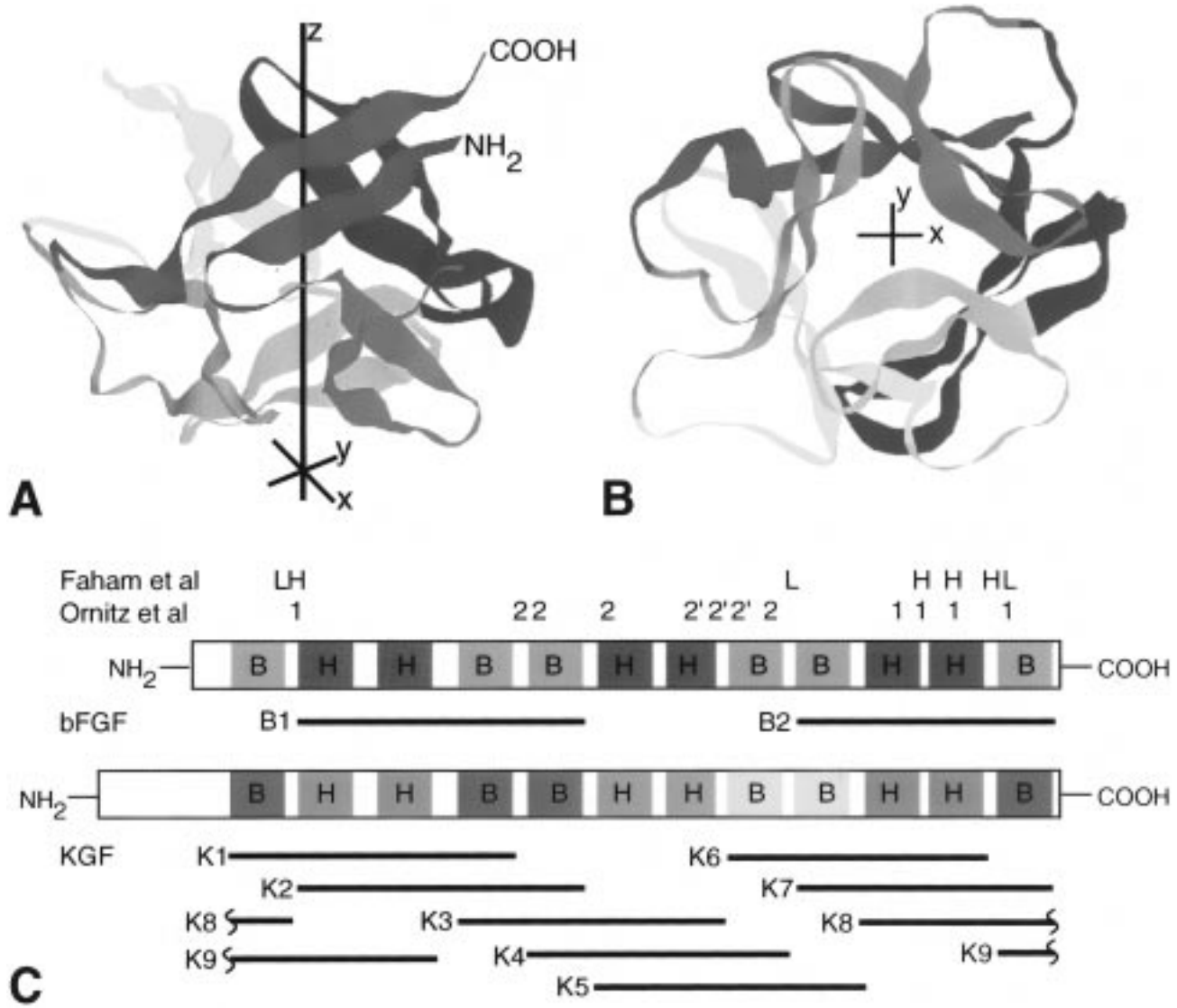

FIGURE 1: Theoretical 3D model of the KGF structure and synthetic peptide design strategy. **(**A**)** Side view of the 3D model of KGF created using the crystallographic coordinates of bFGF, KGF and bFGF sequence alignment, and LOOK molecular modeling software. The barrel sits above three hairpin loops, which fold inward toward the axis of symmetry, oriented vertically. The three barrel components are colored red, green, and yellow. The regions of the KGF sequence contained in these structures are denoted with the same colors in panel B. **(**B**)** Bottom view of the 3D model of KGF shown in panel A, where the axis of symmetry has been rotated 90° so that it is perpendicular to the plane of the page. The three hairpin loops are colored blue, orange, and violet. The regions of the KGF sequence contained in these structures are denoted with the same colors in panel C. **(**C**)** Schematic diagram of the strategy used for peptide selection. Each third of the β-trefoil consists of a BHHB motif, and the arrangement of B and H components for bFGF (top bar) and KGF (bottom bar) are superimposed on the linear protein sequence from amino (left) to carboxyl terminus (right). Peptides K1−9, B1, and B2 precisely span the structural components depicted directly above in the respective schematics. The positions of amino acid residues implicated in bFGF−heparin interaction by Faham and co-workers (*31*) and Ornitz and co-workers (*30*) are indicated above bFGF; residues were classified as primary (1; *30*) or high-affinity (H; *31*) and secondary (2 or 2′; *30*) or low-affinity (L; *31*).

β-sheets. The motif HBBH was not synthesized because the model predicts that the two hairpin regions do not interact with each other. K1 is composed of the amino-terminal BHHB, K2 is composed of HHBB, K3 is composed of BBHH, and so forth. K7 is composed of the BHHB motif at the carboxyl terminus of KGF. K8 and K9 were synthesized by connecting the carboxyl- and amino-terminal barrels with the sequence valine-alanine-valine (VAV), which links the second and third barrel strands. The KGF peptides K2 and K7 correspond to two bFGF peptides identified by Baird and co-workers (*33*) as having heparin and receptor binding activities, and coincidentally also precisely span the motifs HHBB and BHHB, respectively (Figure 1C). In our study, these two bFGF peptides (designated B1 and B2; defined in Table 1) were also synthesized and their properties were compared with those of K1−9.

Heparin Binding by KGF Peptides. The ability of KGF and peptides K1−9, B1, and B2 to bind biotinylated heparin is shown in Figure 2. Peptides K1 and K7−9 bound substantially more heparin than the other peptides tested, suggesting that heparin binding is localized to the amino and carboxyl termini of the KGF molecule. To compare relative affinities of the interactions between the peptides and biotinylated heparin, increasing concentrations of NaCl were added to the reaction mixture (Figure 2A). Higher concentrations of NaCl were associated with decreased heparin binding, and the displacement patterns for peptides K1 and K7−9 were not substantially different from that of KGF.

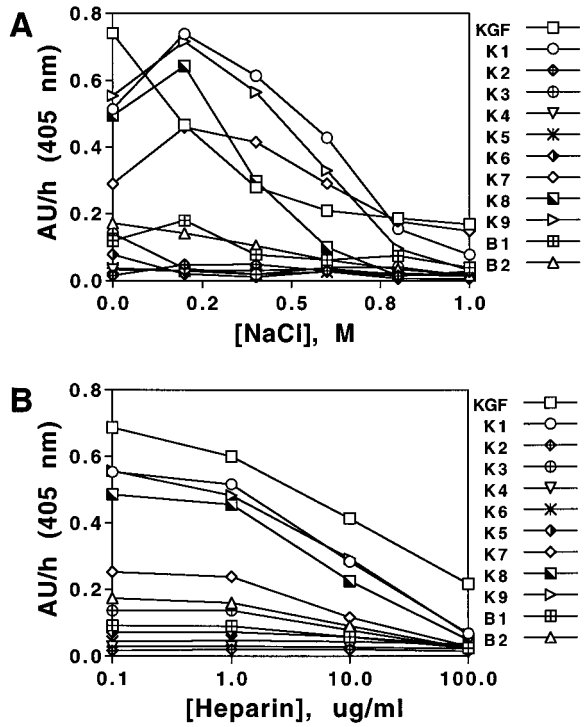

FIGURE 2: Heparin binding by peptides K1−9, B1, and B2. **(**A**)** Peptides were adsorbed to polyvinlyl microtiter plates and the binding of biotinylated heparin was detected using a streptavidin−alkaline phosphatase conjugate and the substrate PNPP. The ordinate shows the rate of absorbance per hour at 405 nm measured over 2 h. The abscissa shows the concentration of NaCl used to wash the plate after incubation and before detection. Where not shown, standard errors from replicate wells are smaller than the symbol size. Results shown are representative of at least three separate experiments. **(**B**)** Peptides adsorbed to microtiter plates were incubated with b-heparin in the presence of various concentrations of soluble heparin, as indicated on the abscissa, and processed as described in panel A. Where not shown, the error bars are smaller than the symbol size. Results shown are representative of at least three separate experiments.

The specificity of interaction between heparin and the peptides was assessed by adding unlabeled heparin to compete for binding with b-heparin (Figure 2B). Unlabeled heparin at a 500-fold excess completely displaced binding of b-heparin to the peptides that showed significant heparin binding.

To identify heparin binding regions of KGF with higher resolution, 65 different 18mer peptides scanning the entire predicted β-trefoil of KGF were synthesized in, and left covalently bound to, special 96-well microtiter plates. Starting with the first 18 residues of K1 in the first well, 18mer peptides in successive wells began by shifting two amino acids toward the carboxyl terminus of the KGF sequence. The bFGF sequence was scanned similarly for comparison with KGF. On the abscissa of Figure 3, the position number refers to the peptide sequence starting position within the β-trefoil. The peptide at position 0 starts at Gly62 and ends at Ile79 for KGF, and starts at Ile26 and ends at Ile43 for bFGF. After position 112, the peptide sequences wrapped around to the amino terminus in the same manner as peptides K8 and K9. For bFGF, strong heparin binding was sustained from position 75 through the carboxyl terminus and wrapped around to position 2 in the amino terminus, while scattered heparin binding was observed from position 20 through 54 (Figure 3, upper panel). KGF also

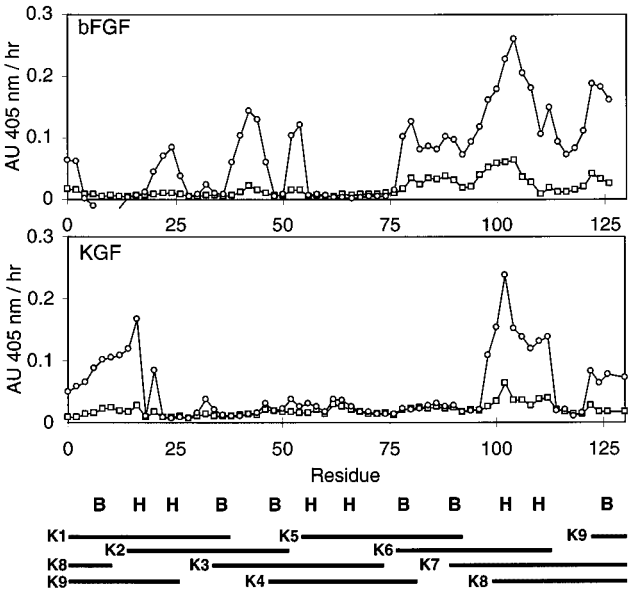

FIGURE 3: Heparin binding by overlapping 18mer peptides spanning the bFGF (upper panel) or KGF (lower panel) sequence. Peptides were synthesized in, and permanently bound to, special 96-well microtiter plates, and the binding of b-heparin was detected using a streptavidin−alkaline phosphatase conjugate and PNPP. The ordinate in each panel shows the rate of absorbance per hour at 405 nm measured over 2 h. Symbols indicate the position of the first residue of each peptide in the growth factor sequence. The peptide at position 0 starts at Gly62 and ends at Ile79 for KGF, and starts at Ile26 and ends at Ile43 for bFGF. After position 112, the peptide sequences wrapped around to the amino terminus in the same manner as peptides K8 and K9. The relative positions of peptides K1−9 are shown below for comparison. Results shown are representative of at least three separate experiments.

showed pronounced and sustained heparin binding at the carboxyl and amino termini, starting at position 94 or the fifth hairpin region, wrapping around to the N terminus and ending at position 16 (Figure 3, lower panel). These data implicate the carboxyl-terminal HHB motif of both KGF and bFGF as well as the N-terminal BHH and BH motifs of KGF and bFGF, respectively, in heparin binding. (Note that implicated regions span the area from the starting position number to 18 residues downstream.)

We observed that heparin binding by four 18mer peptides was relatively low in both bFGF and KGF starting between residues 112−118 in the numbering scheme shown in Figure 3. The consecutive residues Gln-Lys in this region are conserved in bFGF and KGF, and the Lys in bFGF reportedly binds heparin (*19*, *20*). Since the 18mer peptides that start just upstream of this point contain those residues and showed high levels of heparin binding, the occurrence of the Gln-Lys at or near the end of the peptide may negatively affect its interaction with heparin. This could arise from added flexibility or the proximity of the amino-terminal charge, neither of which might occur when this motif was in the middle of the peptide sequence.

To study the contribution to heparin binding of individual amino acid residues implicated in heparin−bFGF interaction by Thompson et al. (*41*), Faham et al. (*31*), and Ornitz et al. (*30*), a subset of these residues were individually changed to alanine in the 18mer peptides. The bFGF sequence K120RTGQYKLGSKTGPGQKA137 (position 102 in Figure 3, upper panel) was synthesized with the following mutations: K120A, R121A, Q124A, K126A, K130A, Q135A,

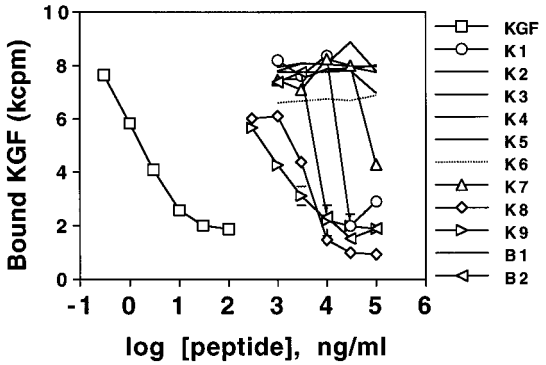

FIGURE 4: Competition for [^{125}I]KGF binding to NIH3T3−KGFR transfectants. The abilities of unlabeled KGF or peptides K1−9, B1, or B2 to displace [^{125}I]KGF from its cell surface receptor were measured as described in Experimental Procedures. Symbols are shown only for peptides which displaced binding. Where not shown, the error bars are smaller than the symbol size. Results shown are representative of at least three separate experiments.

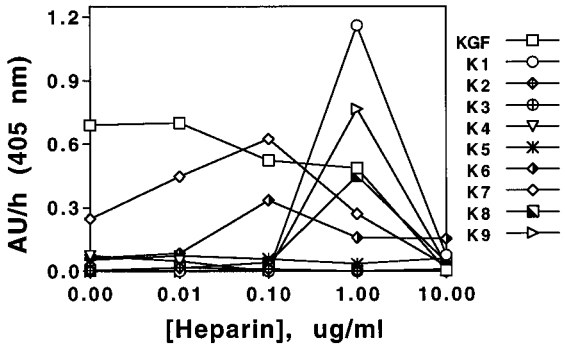

FIGURE 5: Recognition of peptides K1−9 and KGF by the neutralizing monoclonal antibody 1G4. Peptides adsorbed to microtiter plates were incubated with 1G4 in the presence of various concentrations of soluble heparin, as indicated on the abscissa, and the amount of 1G4 bound was determined using a goat anti-mouse IgG−alkaline phosphatase conjugate and PNPP. The ordinate shows the rate of absorbance per hour at 405 nm measured over 2 h. Where not shown, standard errors from replicate wells are smaller than the symbol size. Results shown are representative of at least three separate experiments.

and K136A. The corresponding KGF sequence, N168QKGIPVRGKKTKKEQKT185 (position 106 in Figure 3, lower panel), was synthesized with the following mutations: N168A, Q169A, K170A, V174A, R175A, K177A, K178A, K180A, K181A, Q183A, and K184A. These 18mer peptides were synthesized on the same 96-well plates used to scan the β-trefoil and heparin binding was determined in the same way. The heparin binding ability of the peptides was not significantly reduced by any single amino acid mutation (data not shown). Alanine substitution of all of the residues implicated in the bFGF−heparin cocrystallization studies (K130, R131, K136, Q145, and K146) resulted in a 60% decrease in heparin binding, and when the two remaining basic residues not implicated in the cocrystallization studies, Q134 and K140, were also changed to alanine, a decrease of 90% was observed. Similarly, when all the basic residues in the KGF peptide were changed to alanine, heparin binding decreased 80%.

Interaction of KGF Peptides with the KGFR. We have shown previously that KGF binds to the KGFR tyrosine kinase primarily via residues in the carboxyl-terminal portion of the third IgG domain of that receptor (*37*, *42*). In this study we tested the ability of peptides K1−9, B1, and B2 to displace [^{125}I]KGF from the KGFR expressed on NIH3T3−KGFR transfectants to localize the KGFR binding site on KGF (Figure 4). Displacement by unlabeled KGF was 50% at about 2 ng/mL as reported previously (*38*). K1, K8, K9, and B2 displaced [^{125}I]KGF in a dose-dependent manner; K7 also showed about 50% displacement, but only at the highest concentration tested. While it is obvious from these data that far higher peptide concentrations (10^3−10^4-fold) were required relative to full-length KGF, the fact that several peptides had no effect on KGF binding even at the highest concentrations tested suggests that KGF displacement by K1, K8, K9, and B2 was specific (Figure 4). It is also worth noting that full-length bFGF has been shown to compete effectively for [^{125}I]KGF binding to the KGFR at concentrations approximately 100-fold higher than KGF (*38*). Thus while bFGF may not be a physiologically relevant ligand for the KGFR, we anticipated that a bFGF peptide, such as B2, might demonstrate better [^{125}I]KGF displacement than peptides from regions of KGF outside of the receptor binding site. Experiments designed to test whether K1, K4, and K7, which span the entire KGF β-trefoil, could together reconstitute the displacement potency of KGF were negative in that displacement was no more effective than with K1 alone (data not shown).

Heparin-Dependent Recognition of KGF Peptides by 1G4. A second approach to localizing the receptor binding site of KGF involved identifying the epitope recognized by the KGF-specific neutralizing monoclonal antibody 1G4. This analysis was conducted with the assumption that 1G4 neutralizes KGF activity by a competitive, as opposed to allosteric, mechanism. Two methods were developed to generate comprehensive comparisons of peptides K1−9. The first method was an ELISA in which the peptides were adsorbed to 96-well microtiter plates and 1G4 recognition was detected using a secondary antibody conjugated to alkaline phosphatase. As expected, KGF was easily recognized, and to make the assay sensitive enough to detect peptide recognition without saturating KGF recognition, far less KGF (1000-fold) was adsorbed to the wells than peptide. Interestingly, only KGF and K7 were recognized by 1G4 under these conditions (Figure 5). Extensive testing of incubation conditions revealed that added soluble heparin enhanced the recognition of K7, so the assay was performed across a wide range of heparin concentrations. K7 recognition was maximal at 0.1 μg/mL heparin, while the recognition of K8, K9, and K1 required heparin and showed a biphasic pattern with maximum recognition at 1.0 μg/mL heparin (Figure 5).

The second method of localizing the 1G4 binding epitope on KGF differed from the ELISA scheme in that the peptides were immobilized on PVDF membrane, then probed for 1G4 recognition in a manner similar to immunoblotting with chemiluminescent detection. Dot blots of peptides and full-length proteins were blocked and preincubated with varying concentrations of heparin before probing with 1G4. Figure 6 shows that recognition of KGF by 1G4 does not require heparin but is enhanced by increasing heparin concentrations in this assay. Similar to the results of the ELISA, recognition of K8, K9, and K1 by 1G4 required heparin and displayed a biphasic response to heparin concentration (Figure 6). Recognition did not occur in the absence of heparin, reached

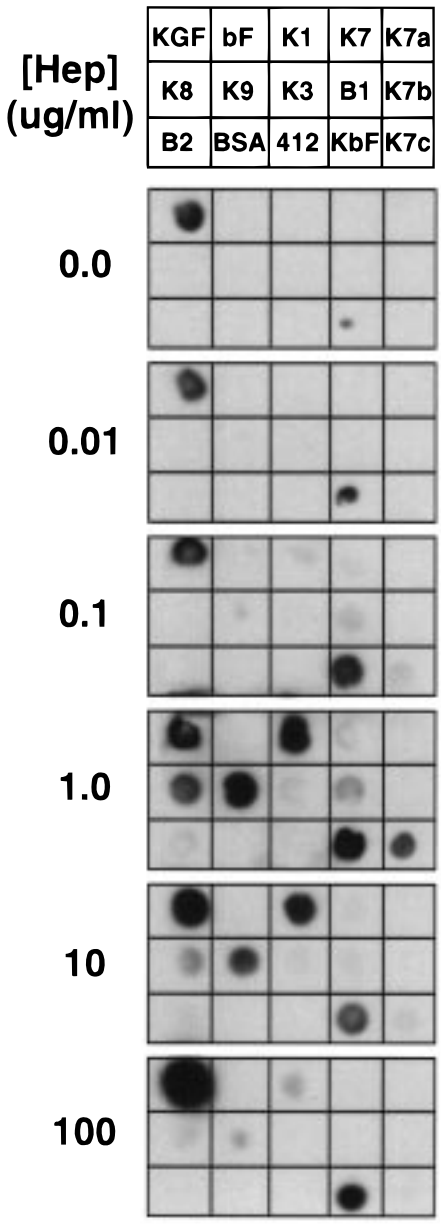

FIGURE 6: Recognition of selected KGF peptides and proteins by the neutralizing monoclonal antibody 1G4. Peptides or proteins immobilized on PVDF membrane were incubated with 1G4 in the presence of various concentrations of soluble heparin, as indicated at the left of each panel, and the amount of 1G4 bound was detected using the ECL chemiluminescence system (Amersham). The top panel shows the position of each peptide or protein tested in lower panels. bF is bFGF. K7a−c are subdomains of K7 (see Results). 412 is a control (KGFR) peptide. KbF is a chimeric protein[3] of KGF and bFGF (see Results). All other designations are as used throughout the text. Equal adsorbance of peptides and proteins was verified by colloidal Coomassie Blue staining of membranes loaded in parallel. Results shown are representative of at least three separate experiments.

a maximum at a heparin concentration of 1 μg/mL, and then decreased as more heparin was added. Peptides K2−6 were not detected by 1G4 under any conditions tested (data not shown). In contrast to the ELISA results, K7 was occasionally detected but only at 1 μg/mL heparin. To investigate this further, portions of K7 were synthesized and tested separately. K7 contains the carboxyl BHHB motif in the KGF sequence, while K7a contains HH, K7b contains HHB, and K7c contains BHH components of the parent motif.

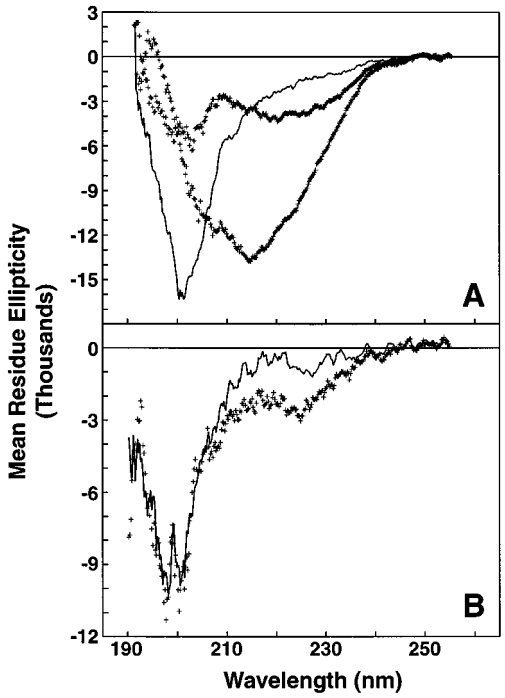

FIGURE 7: CD analysis of heparin−K7 interactions. Mean residue ellipticity, as defined in Experimental Procedures, is shown on the *Y*-axis, and the ultraviolet wavelength (nanometers) is shown on the *X*-axis. The data shown are representative of at least three separate experiments. **(**A**)** CD sprectrum of peptide K7 in the absence (solid line) and presence of heparin at 40 μg/mL (upper hatched line) and 150 μg/mL (lower hatched line). **(**B**)** CD spectrum of KGF K7a, corresponding to the hairpin loop portion of peptide K7, in the absence (solid line) and presence (hatched line) of heparin at 40 μg/mL.

Interestingly, K7c was recognized by 1G4 only in the presence of 1 μg/mL heparin (Figure 6). Peptide 412, identified previously as part of the KGFR sequence that binds directly to KGF (*37*), was included here as a negative control, as were bFGF and BSA. A chimeric molecule[3] containing the amino- and carboxyl-terminal BHHB motifs of KGF and the central BHHB motif of bFGF was also recognized by 1G4 in this assay, and like KGF, recognition was enhanced with increasing heparin concentrations (Figure 6).

Heparin-Induced Folding of KGF Peptides. The ability of heparin to modulate antibody recognition of peptides K1 and K7−9 suggested that heparin may induce the folding of these peptides into a KGF-like conformation. To explore this possibility, we examined the structure of the heparin-binding KGF peptides in the absence and presence of heparin by CD spectroscopy. CD spectra indicated that peptide K7 alone lacked ordered structure (Figure 7A, solid line) but folded into β-sheet in the presence of heparin (Figure 7A, hatched lines). This effect showed a limited dependence on heparin concentration, as shown by the CD spectra of K7

[3] A cDNA encoding a chimeric human KGF−bFGF molecule comprised of the amino terminus of bFGF through the end of the amino-terminal BHHB motif (residues NH_2-MAAGS...LQLQA-COOH), the central BHHB motif of KGF (residues NH_2-VAVGI...LILEN-COOH), and the C-terminal BHHB motif of bFGF (residues NH_2-HYNTY...M-SAKS-COOH) was constructed and expressed in bacteria. Expressed protein was partially purified by heparin−TSK HPLC after elution with a linear gradient of NaCl. A manuscript describing the construction, expression, purification, and biological properties of this chimeric molecule is in preparation (P. J. Kim et al.).

with 40 μg/mL heparin versus 150 μg/mL heparin in Figure 7A. CD data could not be obtained for peptides K1, K8, K9, or B2, which also displayed heparin binding, due to the formation of a precipitate after the addition of heparin. The formation of precipitate was not observed when heparin was added to other peptides that did not bind heparin in other assays, and thus appeared to be a sequence-specific effect. Precipitate formation was also concentration-dependent; i.e., it appeared to occur only at (or above) the peptide concentrations required for CD analysis (100 μg/mL). As controls, we also examined the effects of heparin on peptides K3 and K4, which did not bind heparin in any of the assays used in this study. The CD spectrum of K3 alone suggested the presence of β-sheet, and this was unaffected by heparin addition (data not shown). Peptide K4 did not appear to have any ordered structure in the presence or absence of heparin (data not shown). Together these results strongly suggest that the heparin-induced β-folding displayed by peptide K7 was sequence-specific.

We further analyzed the heparin-induced folding of peptide K7 to identify the minimum sequence required for this effect. Peptides K7a−c were analyzed by CD spectroscopy separately in the absence and presence of heparin. Of these, heparin (40 μg/mL) induced the folding of peptide K7a, spanning the hairpin loop (HH) motif (Figure 7B). Interestingly, the peptides containing portions of barrel strand (BHH and HHB) slowly precipitated upon heparin addition, causing a significant loss of CD signal intensity. Consistent with their role in establishing the β-trefoil fold, each portion of barrel strand (B) contains three medium or large hydrophobic residues. While it is unclear why K7 remained in solution in the presence of heparin, it appeared that the inclusion of only one barrel strand (B) motif in the shorter peptides resulted in the heparin-induced aggregation of these hydrophobic residues and ultimately precipitation of the peptide−heparin complex. In any case, it is noteworthy that most of the residues implicated in bFGF−heparin interaction also fall into the carboxyl-terminal hairpin loop (HH) region.

DISCUSSION

Several studies have identified amino acids in bFGF involved in heparin binding (*33*−*35*, *43*−*46*). These studies exploited a variety of strategies, converging on the amino- and carboxyl-terminal regions of the bFGF sequence. Through extensive site-directed mutagenesis, key amino acids involved in heparin binding were identified by Thompson et al. (*41*) as K27, N28, R82, K120, R121, T122, Q124, K126, K130, Q135, and K136. Of these, K27, N28, R121, K126, Q135, and K136 were also identified in cocrystallization studies (*30*, *31*), the positions of which are indicated in the linear bFGF schematic in the upper portion of Figure 1B. Residues R121, K126, Q135, and K136 fall within the carboxyl-terminal HHB motif, while K27 and N28 fall within the amino-terminal BH motif. Both Thompson et al. (*30*) and Ornitz et al. (*41*) identified several other residues in the central BHHB motif as secondary sites of heparin interaction. In our assays, peptides B1 and B2 bound biotinylated heparin and were well-retained on heparin−TSK. In addition, scanning bFGF with 65 different 18mer peptides implicated the carboxyl-terminal HHB motif as well as the amino-terminal BH motif in heparin binding. The consistency of these results with the published studies of bFGF was an important validation of our methodology as we extended our investigation to KGF.

Peptides K1 and K7−9 bound substantially more heparin than the other KGF peptides tested, suggesting that heparin binding residues are confined to the amino and carboxyl termini of the KGF sequence. Salt extraction of the heparin from these peptides suggested that the displacement patterns for peptides K1 and K7−9 were not substantially different from that of KGF. Consistent with these findings, K7 exhibited 90% of the retention time of full-length KGF on heparin−TSK affinity chromatography, and K1, K8, and K9 were also significantly retained (Table 1). In contrast, K3−5, which span the central portion of the KGF sequence from the second to the fifth barrel strands, showed no heparin binding by ELISA and were not retained by heparin−TSK (Table 1). The absence of heparin binding residues in the central third of KGF, in contrast to bFGF, may explain the lower affinity of KGF for heparin relative to bFGF (*1*). Since peptide K5 overlaps the first barrel strand of K7, the heparin binding observed for K7 may be attributable to the carboxyl-terminal HHB portion of that peptide. This conclusion is also supported by the results of scanning the entire predicted β-trefoil of KGF with 65 different 18mer peptides, which indicated that the carboxyl-terminal HHB and amino-terminal BHH motifs of KGF contain heparin binding sites. As for aFGF and bFGF, these regions are juxtaposed in the theoretical KGF structure (Figure 1A,B).

The contribution to heparin binding of individual amino acid residues implicated in the cocrystallization of bFGF with oligosaccharides (*30*, *31*) was assessed by changing these residues individually to alanine in the 18mer peptides in bFGF, and in the corresponding region of KGF. Somewhat surpisingly, the heparin binding ability of the peptides was not significantly reduced by any single amino acid mutation, although grouped changes (e.g., K120, R121, K126, Q135, and K136) in bFGF decreased heparin binding significantly. Although a substantial decrease was observed when 10 of 18 residues in the KGF peptide were changed to alanine, further information about the contributions of residues in this region of KGF may require an extensive series of grouped (two- or three-residue) changes.

Interestingly, K1, K8, K9, and B2 specifically displaced [^{125}I]KGF from cell-surface KGFR in a dose-dependent manner, and K7 showed 50% displacement at the highest concentration tested. Thus, the same group of peptides that bound heparin also blocked KGF−KGFR interaction. The ability of B2 to block KGF binding was anticipated on the basis of previous evidence (*29*, *33*), and the ability of bFGF to bind to the KGFR with low affinity (*38*). As in the heparin binding assays, these results also supported the validity of results obtained with KGF peptides. A second approach used in this study to localize the receptor binding site of KGF involved identifying the epitope recognized by the KGF-specific neutralizing monoclonal antibody 1G4. In an ELISA in which peptides K1−9 were adsorbed to polyvinyl microtiter plates, only KGF and K7 were recognized by 1G4 in the absence of added heparin. Heparin enhanced K7 recognition, and was required for recognition of K8, K9, and K1.

The 1G4 binding epitope on KGF was also investigated using peptides and proteins immobilized on PVDF membrane. Consistent with the ELISA results, recognition of

K8, K9, and K1 by 1G4 required heparin. In contrast to the ELISA, K7−1G4 interaction was not reliably detected. A portion of K7 containing the first barrel strand and hairpin loop (BHH) of the parental BHHB motif was recognized by 1G4, but only in the presence of heparin. In addition, a chimeric molecule[3] containing the amino- and carboxyl-terminal BHHB motifs of KGF and the central BHHB motif of bFGF was also recognized by 1G4 in this assay, and recognition was enhanced with added heparin. bFGF, in contrast, was not recognized under any conditions. Since peptides K1 and K7−9 overlap either one or both strands of the barrel component formed by the N and C termini (Figure 1), the 1G4 binding epitope may bridge these two antiparallel strands somewhere along their length. 1G4 recognition of peptide K7c suggests that this may occur at the end of the C-terminal barrel strand where it adjoins the C-terminal hairpin loop. When the 3D model of KGF is viewed as a space-filling structure, this putative 1G4 binding epitope can be observed as a well-delimited contiguous surface (not shown).

That this region of KGF may be involved in receptor interaction is suggested by the fact that 1G4 binding blocks this interaction (*27*, *47*). Moreover, corresponding sites have been implicated as receptor binding sites in bFGF. Primary sites of bFGF−FGFR interaction have been identified by structure-based site-directed mutagenesis as Y24, Y103, L140, M142, R44, and N101 (*29*). Of these, four are in the carboxyl-terminal BHHB motif and two are in the amino-terminal barrel strand and adjoining hairpin loop. Secondary receptor binding sites identified in the same study are K110, Y111, and W114; these are all in the carboxyl-terminal BH motif of bFGF (*29*). The universality of this region as critical for receptor recognition in FGFs is supported by the work of Seddon et al. (*48*). That study demonstrated that the region joining the first carboxyl-terminal barrel strand with the carboxyl-terminal hairpin loop of aFGF (residues 118−122), when substituted into the corresponding region of bFGF, increased the range of the receptor binding specificity of bFGF to include high-affinity binding to the KGFR. Two secondary receptor binding sites identified by Springer et al. (*29*) in bFGF, K110 and Y111, fall within this region of aFGF. Evidence implicating the amino-terminal regions of KGF and bFGF in receptor recognition was reported by Ronit Reich-Slotky et al. (*49*), who observed that KGF−bFGF chimeras possessing the amino terminus of KGF failed to stimulate DNA synthesis in NIH3T3 cells, whereas the reciprocal chimeras showed substantial activity on this cell type. These and other studies indicate that the carboxyl- and amino-terminal BHHB motifs of bFGF contain most of the residues involved in both heparin and receptor binding, and suggest that these may be functionally important regions generally among FGF family members.

In a previous investigation of the KGF binding site on the KGFR, we observed that 1G4−KGF interaction in solution was unaffected by added heparin, suggesting that the 1G4 and heparin binding sites on KGF do not overlap (*37*). Others have reported that heparin does not induce conformational changes in soluble KGF (*50*). However, added heparin clearly modulated the patterns of 1G4 binding observed in the ELISA and PVDF blot assays used here. In the ELISA, KGF recognition decreased with increasing heparin concentrations, while on PVDF, the opposite pattern was seen. While the differences between these assays may be specific to the immobilizing surface (polyvinyl vs PVDF), heparin clearly altered the binding of 1G4 to immobilized, but not soluble KGF. Given that KGF is also immobilized by target cell surfaces in vivo, the heparin modulation of 1G4 binding observed here may have biological relevance. Heparin-dependent 1G4 recognition of KGF peptides probably resulted from heparin-induced peptide folding into a more KGF-like conformation and, from a practical standpoint, helps to define a minimum functional unit of KGF−heparin interaction.

Heparin-induced peptide folding is suggested by structural analyses of the heparin-binding KGF peptides by CD, which indicated that, while none had ordered structure in solution alone, K7 folded into β-sheet in the presence of heparin. That this folded peptide conformation more closely resembled KGF is suggested by specific 1G4 recognition under these conditions. A similar folding of peptides K1, K8, and K9 was not observed; these peptides were precipitated from solution by heparin at the high peptide concentrations needed for CD analysis. Heparin-induced conformational changes may have exposed hydrophobic residues in their respective barrel strands, facilitating peptide aggregation and precipitation. Three such residues in each barrel strand are normally buried together in the core of the β-trefoil fold (*36*). Why the K7−heparin complex did not precipitate is unclear, but it was exceptional in this regard. Heparin-induced folding of peptide K7a suggests that only the carboxyl-terminal hairpin loop is required to observe this effect. Together with the results of the other heparin binding assays, these data further localize the heparin binding sites in the KGF carboxyl terminus to residues between positions 157 and 185, or the carboxyl-terminal hairpin loop (Figure 1A−C, identified by the color violet).

One of the aims of this study was to determine if the three parts of the KGF β-trefoil could stand alone, structurally and/or functionally. The folding of K7 suggests that this can be achieved, to some degree, in the presence of heparin. The effects of heparin-folded K7 on KGFR-mediated DNA synthesis were investigated, but these experiments failed to show peptide-attributable agonist or antagonist activity because the heparin required for K7 folding was a potent inhibitor of KGF-stimulated mitogenesis. Nonetheless, the data presented here strongly suggest that this portion of KGF, as well as the-amino terminal region encompassed by peptide K1, contain residues important for both heparin and receptor binding. Our results also reinforce the hypothesis that heparin and receptor binding are mediated by residues within the amino- and carboxyl-terminal hairpin loops generally among FGFs. Overall, the strategy of using synthetic peptides based on a hypothetical structure has succeeded in highlighting regions of KGF for further study, and may be useful for preliminary explorations of other proteins for which structural information on family members is available.

ACKNOWLEDGMENT

We thank Julia Roach and Diane Breckenridge-Miller for technical assistance, and Robert Pearlstein for advice and assistance with molecular modeling.

REFERENCES

1. Rubin, J. S., Osada, H., Finch, P. W., Taylor, W. G., Rudikoff, S., and Aaronson, S. A. (1989) *Proc. Natl. Acad. Sci. U.S.A. 86*, 802−806.
2. Finch, W. P., Rubin, J. S., Miki, T., Ron, D., and Aaronson, S. A. (1989) *Science 245*, 752−755.
3. Rubin, J. S., Bottaro, D. P., Chedid, M., Miki, T., Ron, D., Cheon, G., Taylor, W. G., Fortney, E., Sakata, H., Finch, P. W., and LaRochelle, W. J. (1995) *Cell Biol. Int. 5*, 399−411.
4. Rubin, J. S., Bottaro, D. P., Chedid, M., Miki, T., Ron, D., Cunha, G. R., and Finch, P. W. (1995) *EXS 74*, 191−214.
5. Miki, T., Fleming, T. P., Bottaro, D. P., Rubin, J. S., Ron, D., and Aaronson, S. A. (1991) *Science 252*, 72−75.
6. Finch, P. W., Cunha, G. R., Rubin, J. S., Wong, J., and Ron, D. (1995) *Dev. Dyn. 203*, 223−240.
7. Miki, T., Bottaro, D. P., Fleming, T. P., Smith, C. L., Burgess, W. H., Chan, A. M.-L., and Aaronson, S. A. (1992) *Proc. Natl. Acad. Sci. U.S.A. 89*, 246−250.
8. Yamasaki, M., Miyake, A., Tagashira, S., and Itoh, N. (1996) *J. Biol. Chem. 271*, 15918−15921.
9. Emoto, H., Tagashira, S., Mattei, M. G., Yamasaki, M., Hashimoto, G., Katsumata, T., Negoro, T., Nakatsuka, M., Birnbaum, D., Coulier, F., and Itoh, N. (1997) *J. Biol. Chem. 272*, 23191−23194.
10. Post, M., Souza, P., Liu, J., Tseu, I., Wang, J., Kuliszewski, M., and Tanswell, A. K. (1996) *Development 122*, 3107−3115.
11. Ohmichi, H., Koshimizu, U., Matsumoto, K., and Nakamura, T. (1998) *Development 125*, 1315−1324.
12. Bellusci, S., Grindley, J., Emoto, H., Itoh, N., and Hogan, B. L. (1997) *Development 124*, 4867−4878.
13. Finch, P. W., Pricolo, V., Wu, A., and Finkelstein, S. D. (1996) *Gastroenterology 110*, 441−451.
14. Brauchle, M., Madlener, M., Wagner, A. D., Angermeyer, K., Lauer, U., Hofschneider, P. H., Gregor, M., and Werner, S. (1996) *Am. J. Pathol. 149*, 521−529.
15. Nemeth, J. A., Zelner, D. J., Lang, S., and Lee, C. J. (1998) *Endocrinology 156*, 115−125.
16. Canatan, H., Shidaifat, F., Kulp, S. K., Zhang, Y., Chang, W. Y., Brueggemeir, R. W., and Lin, Y. C. (1997) *Endocr. Res. 23*, 311−323.
17. Leung, H. Y., Mehta, P., Gray, L. B., Collins, A. T., Robson, C. N., and Neal, D. E. (1997) *Oncogene 15*, 1115−1120.
18. Rapraeger, A. C., Guimond, S., Krufka, A., and Olwin, B. B. (1994) *Methods Enzymol. 245*, 219−240.
19. Ornitz, D. M., and Leder, P. (1992) *J. Biol. Chem. 267*, 16305−16311.
20. Ron, D., Bottaro, D. P., Finch, P. W., Morris, D., Rubin, J. S., and Aaronson, S. A. (1992) *J. Biol. Chem. 268*, 2984−2988.
21. Gospodrowicz, D., Plouet, J., and Malerstein, B. (1990) *J. Cell. Physiol. 142*, 325−333.
22. Li, M., and Bernard, O. (1992) *Proc. Natl. Acad. Sci. U.S.A. 89*, 3315−3319.
23. Rapraeger, A. C., Krufka, A., and Olwin, B. B. (1991) *Science 252*, 1705−1708.
24. Ornitz, D. M., Yayon, A., Panagan, J. G., Svahn, C. M., Levi, E., and Leder, P. (1992) *Mol. Cell. Biol. 12*, 240−247.
25. Roghani, M., Mansukhani, A., Dell'Era, P., Bellosta, P., Basilico, C., Rifkin, D. B., and Moscatelli, D. (1994) *J. Biol. Chem. 269*, 3976−3984.
26. Yayon, A., Klagsburn, M., Esko, J. D., Leder, P., and Ornitz, D. M. (1991) *Cell 64*, 841−848.
27. Kan, M., Wang, F., Xu, J., Crabb, J. W., Hou, J., and Mckeehan, W. L. (1993) *Science 259*, 1918−1921.
28. Spivak-Kroizman, T., Lemmon, M. A., Dikic, I., Ladbury, J. E., Pinchasi, D., Huang, J., Jaye, M., Crumley, G., Schlessinger, J., and Lax, I. (1994) *Cell 79*, 1015−1024.
29. Springer, B. A., Pantoliano, M. W., Barbera, F. A., Gunyuzlu, P. L., Thompson, L. D., Herblin, W. F., Rosenfeld, S. A., and Book, G. W. (1994) *J. Biol. Chem. 269*, 26879−26884.
30. Ornitz, D. M., Herr, A. B., Nilsson, M., Westman, J., Svahn, C. M., and Waksman, G. (1995) *Science 268*, 432−436.
31. Faham, S., Hileman, R. E., Fromm, J. R., Linhardt, R. J., and Rees, D. C. (1996) *Science 271*, 11116−11120.
32. Herr, A. B., Ornitz, D. M., Sasisekharan, R., Venkataraman, G., and Waksman, G. (1997) *J. Biol. Chem. 272*, 16382−16389.
33. Baird, A., Schubert, D., Ling, N., and Guillemin, R. (1988) *Proc. Natl. Acad. Sci. U.S.A. 85*, 2324−2328.
34. Zang, J., Cousens, L. S., Barr, P., and Sprang, S. R. (1991) *Proc. Natl. Acad. Sci. U.S.A. 88*, 3446−3450.
35. Zhu, X., Komiyo, H., Chirino, A., Faham, S., Fox, G. M., Arakawa, T., Hau, B. T., and Rees, D. C. (1991) *Science 251*, 90−95.
36. Murzin, A. G., Lesk, A. M., and Chothia, C. (1992) *J. Mol. Biol. 223*, 531−543.
37. Bottaro, D. P., Fortney, E., Rubin, J. S., and Aaronson, S. A. (1993) *J. Biol. Chem. 268*, 9180−9183.
38. Bottaro, D. P., Rubin, J. S., Ron, D., Finch, P. W., Florio, C., and Aaronson, S. A. (1990) *J. Biol. Chem. 265*, 12767−12770.
39. King, D. S., Fields, C. G., and Fields, G. B. (1990) *Int. J. Pept. Protein Res. 36*, 255−266.
40. Rosenfeld, S. J., Young, N. S., Alling, D., Ayub, J., and Saxinger, C. (1994) *Arch. Virol. 136*, 9−18.
41. Thompson, L. D., Pantoliano, M. W., and Springer, B. A. (1994) *Biochemistry 33*, 3831−3840.
42. Cheon, H. G., LaRochelle, W. J., Bottaro, D. P., Burgess, W. H., and Aaronson, S. A. (1994) *Proc. Natl. Acad. Sci. U.S.A. 91*, 989−993.
43. Harper, J. W., and Lobb, R. R. (1988) *Biochemistry 27*, 671−680.
44. Eriksson, A. E., Cousens, L. S., Weaver, L. H., and Matthews, B. W. (1991) *Proc. Natl. Acad. Sci. U.S.A. 88*, 3441−3445.
45. Ago, H., Kitagawa, Y., Fujishima, A., Matsura, Y., and Katsube, Y. (1991) *J. Biochem. 110*, 360−369.
46. Eriksson, A. E., Cousen, L. S., and Matthews, B. W. (1993) *Protein Sci. 2*, 1274−1281.
47. Alarid, E. T., Rubin, J. S., Young, P., Chedid, M., Ron, D., Aaronson, S. A., and Cunha, G. R. (1994) *Proc. Natl. Acad. Sci. U.S.A. 91*, 1074−1078.
48. Seddon, A. P., Aviezer, D., Lu-Yan, L., Bohlen, P., and Yayon, A. (1995) *Biochemistry 34*, 731−736.
49. Reich-Slotky, R., Shaoul, E., Berman, B., Graziani, G., and Ron, D. (1995) *J. Biol. Chem. 270*, 29813−29818.
50. Wen, J., Hsu, E., Kenney, W. C., Philo, J. S., Morris, C. F., and Arakawa, T. (1996) *Arch. Biochem. Biophys. 332*, 41−46.

BI9801917